Spatial-SIR with Network Structure and Behavior: Lockdown Policies and the Lucas Critique[‡]

Alberto Bisin Andrea Moro

August 4, 2020

Abstract

We extend a Spatial-SIR model of the diffusion of an infection to include heterogeneous agents interacting socially in three different types of location every day: City, School/Work, and Home. Contagion-risk averse agents respond behaviorally to the diffusion of the epidemic by limiting their social interactions. Firms also respond, by allowing employees to work remotely depending on their productivity. We study the effects of several non-pharmaceutical intervention on epidemic dynamics, e.g. selective lockdowns. Simulations illustrate how the network structure generates local herd immunities along socio-demographic dimensions, affecting policy outcomes. Finally, substantiating a "Lucas critique" argument, we assess the cost of naive policies ignoring the behavioral responses of agents and firms.

[‡]Please check our websites for an updated version of this paper. Bisin: New York University, wp.nyu.edu/albertobisin/, alberto.bisin@nyu.edu . Moro: Vanderbilt University andreamoro.net, andrea@andreamoro.net

1 Introduction

In this paper, we develop and study a model of diffusion of an infection to uncover several stylized facts about the effectiveness of public health policies on the contagion dynamics. More specifically, we construct a Spatial-SIR, along the lines of the model introduced in Bisin and Moro (2020a), and we extend it to allow for several important dimension of the diffusion process:[1] i) a demographic and network structure; ii) behavioral responses of agents and firms to the diffusion of the epidemics and to policy interventions. The spatial dimension accounts for the effects of local herd immunity in the diffusion of the epidemic. We capture the demographic and network structures by modeling different locations where agents interact socially, allowing for heterogeneous rates of diffusion of the epidemic and for heterogeneous effects, e.g., case-fatality-rates. Behavioral responses allow contagion-risk averse agents to reduce their social interactions and firms to instruct their workers to operate remotely depending on their productivity.

Frontier research in epidemiology has proposed models of contagion extending the classic SIR model in many directions, including detailed descriptions of the geographic or network characteristics of the agents' social interactions - see e.g., Eubank et al. (2004) and the research at GLEAM project, mobs-lab, and the Imperial's college MRC Centre for Global Infectious Disease Analysis.[2] While these models appear to fundamentally aim at forecasting with accuracy and precision, their complexity make it difficult to uncover the main driving forces of the epidemics of the effects of polices on it. To understand these driving forces more clearly, and to identify the mechanisms through which non-pharmaceutical interventions operate, we remain methodologically within the confines of stylized models of the diffusion of epidemics.

In the model, which we introduce in Section 2, agents belong to three types: Students/Workers, Adult not employed, and Old. The types differ because of the locations they potentially visit each day. There are three locations: the city, a School/Work location, home, which differ by the density of contacts. Agents may become infected when they get close to the location of an infected agent. We calibrate the model to reproduce several stylized facts about the diffusion of SARS-CoV-2 epidemics. Agent types are calibrated to match the U.S. demographics, particularly the family size distribution by age.

The model identifies several important factors that are relevant in understanding the diffusion of the epidemics, highlighting that local herd immunities may form

[1] The simplest model of epidemic diffusion is the SIR model, from Kermack and McKendrick (1927), Kermack and McKendrick (1932) is formally represented by a system of differential equations describing the flows between three subsets of a population: from Susceptibles into Infected and from Infected into Recovered (which includes the Dead).

[2] Available, respectively, at https://covid19.gleamproject.org, https://www.mobs-lab.org/projects.html, and https://www.imperial.ac.uk/mrc-global-infectious-disease-analysis. Last retrieved: Aug 2, 2020

not only geographically (the focus of our research in Bisin and Moro (2020a)), but also along socio-demographic dimensions depending on the network structure. This structure allows for heterogeneous rates of diffusion of the epidemic and for heterogeneous effects, e.g., case-fatality-rates.

For instance, in our simulations the City originates more infections than School/Work and School/Work more than Home, even though Home is the most dense location and the City is the least dense. This is because the ranking of the locations in terms of density is opposite to the ranking in terms of size and herd immunity is achieved earlier at Home and at School/Work than in the City. Similarly, the fact that the epidemic is largely concentrated on the Young is explained by their exposure at School/Work where there are more contacts than at Home. These effects of local herd immunity are akin to a selection effect, whereby the epidemic spreads selectively by location and demographic structure.

Our analysis also illustrates the relevance of the indirect effects induced by the behavioral responses of agents and firms, across locations and demographic types.[3]

For instance, the behavioral responses of (mostly) the Young, (mostly) in the School/Work location, have a sizable important effect on the Old in the City, where most of the Old get infected.

In Section 3 we use this model to study the effects of several possible public health policy interventions, specifically various lockdown and selected isolation strategies.[4] It identifies clearly how a lockdown strategy interacts in rather subtle ways with the dynamics of herd immunity. When the lockdown is placed too early, the fraction of infected is too small, herd immunity is too far out, and at reopening a second wave of infections reaches a peak higher than the first one. If reopening is delayed to occur at a lower fraction of active cases than the one that triggered the lockdown, a strategy we labeled *cautious reopening*, herd behavior is more advanced at reopening and the second wave is substantially dampened. In addition, the network and demographic strcuture of the model allows us study two selective lockdown policies. In the first one, we limit the lockdown to the City and we let firms/schools decide whether to operate remotely. In the second one, we limit the lockdown to the Old, a policy aiming at reducing total fatalities while bearing limited economic costs (the Old are not economically active, but suffer a higher fatality rate than other demographic groups). Both these lockdown policies have the important property that they are much less costly, economically, as worker/students remain active but this needs to

[3]Several empirical paper have used cellular phone data to document how fear of contagion has affected mobility or show that the economy deteriorated substantially even before or independently of lockdown orders. See, for example, Alfaro et al. (2020), Aum et al. (2020), Barrios et al. (2020), Bartik et al. (2020), Cicala et al. (2020), Coibion et al. (2020), Goolsbee and Syverson (2020), Gupta et al. (2020), Kahn et al. (2020), Rojas et al. (2020).

[4]The spatial dimension of the model allows for the study of test-track-trace interventions, which we have not completed

be traded-off with additional costs in terms of health outcomes at the steady-state or at the peak (e.g., if there is a health care resource constraint, such as hospital/ICU beds). While these selective lockdowns have positive direct effects in terms of economic costs, indirect effects across locations and/or demographic types could in priciple substantially limit their advantage over general lockdowns. This does not appear to happen in our simulations. The City-Only lockdown does not induce a much larger fraction of infected at steady-state than the general lockdown, while the Old-Only lockdown is very successful in limiting Old agents' deaths.

Finally, and most importantly, in Section 4 we illustrate the implications of what economists refer to as the Lucas Critique in the context of epidemiological models. Policy evaluations and interventions disregarding that agents' and firms' "decision rules vary systematically with changes in the structure of series relevant to the decision maker" (Lucas (1976)) might lead to policy decisions which are very costly in terms of their effects on the dynamics of the epidemic. The costs of policies that disregard behavioral responses are clearer if we consider that the lock-down and opening thresholds are calibrated to flatten the infections curve so has to avoid hitting a constraint on the available health care resources. In this case, our simulations imply that health care resources will be under-utilized afterlock-down (that is, the lock-down will turn out to be stricter than necessary) and possibly they will instead be over-run after reopening.

We think of the model we study as the epidemiological component of a more general economic model in which the policy trade-off between economic activity and epidemic diffusion is evaluated, as, e.g., in Atkeson (2020), Alvarez et al. (2020), Jarosch et al. (2020), Kaplan et al. (2020).[5] In the next section we introduce several models in steps, as their complexity increases: adding first a spatial dimension to the basic SIR, then structured demographic and network components, and finally behavioral responses on the part of agents and firms. We do this for a pedagogical reasons, but also because each of partial models are of interest per se, depending on the research questions. We study the effects of different counterfactual health policies only on the full model.

[5]Most of the recent wealth of contributions to the study of the SARS-CoV-2 epidemic in economics has basically restricted its epidemiology component the SIR model. see e.g., Fernandez-Villaverde and Jones (2020), Atkeson (2020), Eichenbaum et al. (2020), Keppo et al. (2020), Weitz et al. (2020), Brotherhood et al. (2020). As exceptions, Antràs et al. (2020) and Glaeser et al. (2020) introduce connections between different geographical units; Acemoglu et al. (2020) and Alfaro et al. (2020) add a demographic structure like we do; and Azzimonti et al. (2020) adds a network structure. Ellison (2020) allow for heterogeneity of the contact process between subpopulations.

2 Epidemic by Spatial, Demographic, Network, and Behavior Characteristics

In this section we introduce a model of the dynamics of an epidemics which, while stylized, contains several important components needed to analyze the effects different forms of lockdowns. We build on the Spatial-SIR we have studied in Bisin and Moro (2020a) by allowing i) for heterogeneity in agents' type and in the characteristics of the (social) spaces where they interact; and ii) for behavioral responses of risk-averse agents and forms.

Specifically, we enlarge the agents' type-space to account for age-structure and occupation status; moreover, we enrich the (social) spacial structure to account for agents' social interactions in distinct networks. We model agents responding to the dynamics of the epidemic, by choosing to limit their social contacts, and we assume that some schools/firms adopt behavioral responses similar to the agents', that is, they choose to shut down operations or to allow workers to work remotely, to limit infections in the school/workplace.

2.1 The Spatial-SIR Model

The Spatial-SIR model in Bisin and Moro (2020a) is a SIR model in which agents interact locally in a two-dimensional space. The dynamics of an infection in this model differ from those in the standard SIR. The fundamental differences can be rationalized in terms of the effects of local interactions which give rise to *matching frictions* (implicitly defined by geography and people's movements), in turn inducing a form of *local herd immunity*. Local herd immunity slows down the diffusion of infection in the early stages and accelerates it afterwards (as aggregate herd immunity is delayed).[6]

Agents are located in space, e.g., a lattice, which we call "the City." Agents are ex-ante identical in terms of demographic characteristics and symmetric in terms of location in space. Two agents come into contact when they are at a geographical distance in space closer than p. Agents move randomly in space: Every day $t = [0, T]$, agents travel distance μ toward a random direction of $d \sim U[0, 2\pi]$ radians.[7] Spatial-SIR is represented by the following transitions: i) a Susceptible agent in a location within distance p from the location of an Asymptomatic becomes infected with probability π;[8] ii) an Asymptomatic agent infected at t, at any future period, can become sYmptomatic with probability ν, or can Recover with probability ρ; iii)

[6] This Section (including the Figures) is taken verbatim from Bisin and Moro (2020a).

[7] When they get close to the boundary, the direction is randomly drawn but constrained to point opposite to the boundary.

[8] Susceptible agents are not infected upon contact with a sYmptomatic agent; this is to capture the fact that sYmptomatic agents are either isolated at home or in the hospital

an agent who has become sYmptomatic at t, at any future period, can Recover with probability ρ, or can Die with probability δ; iv) Dead and Recovered agents never leave these states (this assumes Recoved agents are immune to infection).[9]

We calibrate transitions away and between the infected states, A, Y, D, R to various SARS-CoV-2 parameters from epidemiological studies, notably e.g. Ferguson et al. (2020). We calibrate the model from estimates of initial (prior to policy interventions) growth rates of the epidemics (in Lombardy, Italy) and data on average contacts in Mossong et al. (2008).[10] Figure 1 illustrates the dynamics of the epidemic in space at the calibrated parameters, from the location of the outbreak.[11]

2.2 The Structured Spatial-SIR

We extend the Spatial-SIR model introducing three *types of* locations: the *City* at large, a set of *School/Work* locations that are denser than the city, and shared by subsets of agents, and several *Home* locations shared by agents that belong to the same family. We let agents differ, by age and occupation, in their access to these three types of locations. Our goal is to maintain a parsimonious structure while replicating features of general epidemics that are relevant for policy analysis, to produce relatively robust results in a stylized model. The age-structure of the population has specific relevance for the SARS-CoV-2 epidemic, because the case-fatality-rate is very skewed, higher for older agents. Moreover, the age-structure interacts with the location structure, as older agents tend not to visit School/Work and hence interact mostly at Home.

The first type of agents are labeled *Young*, and represent workers/students. These agents spend part of their day in School/Work, that is, in a location where they interact daily with the same individuals. These locations have a higher population density than the city at large. The second type of agents are labelled *Not employed,* represent adult individuals below 65 years of age that do not have access to a School/Work location. The third type of agents are the *Old*, representing agents who are not working as well, but we want to distinguish from younger not employed individuals because of their higher fatality rate and because they tend to live at home with individuals of the same type.

Each day is divided in three periods and each period is dedicated to a location where agents interact: Period 1 is devoted to visiting the City, Period 2 to visiting the School/Work location and Period 3 to stay at Home. However, agents might choose or be structurally restricted from visiting the City and/or School/Work and hence

[9] The resulting dynamical system is difficult to characterize formally. In the Appendix of Bisin and Moro (2020a) we show that it can be written as a Markov chain on configurations in space, along the lines of interacting particle system models (Liggett, 2012; Kindermann and Snell, 1980).

[10] See Appendix for the details on the calibration.

[11] All our simulations, for all parameter values and initial conditions, converge to a unique distribution over the state space $[S, A, Y, R, D]$.

Figure 1: Geographic progression of infections and recoveries

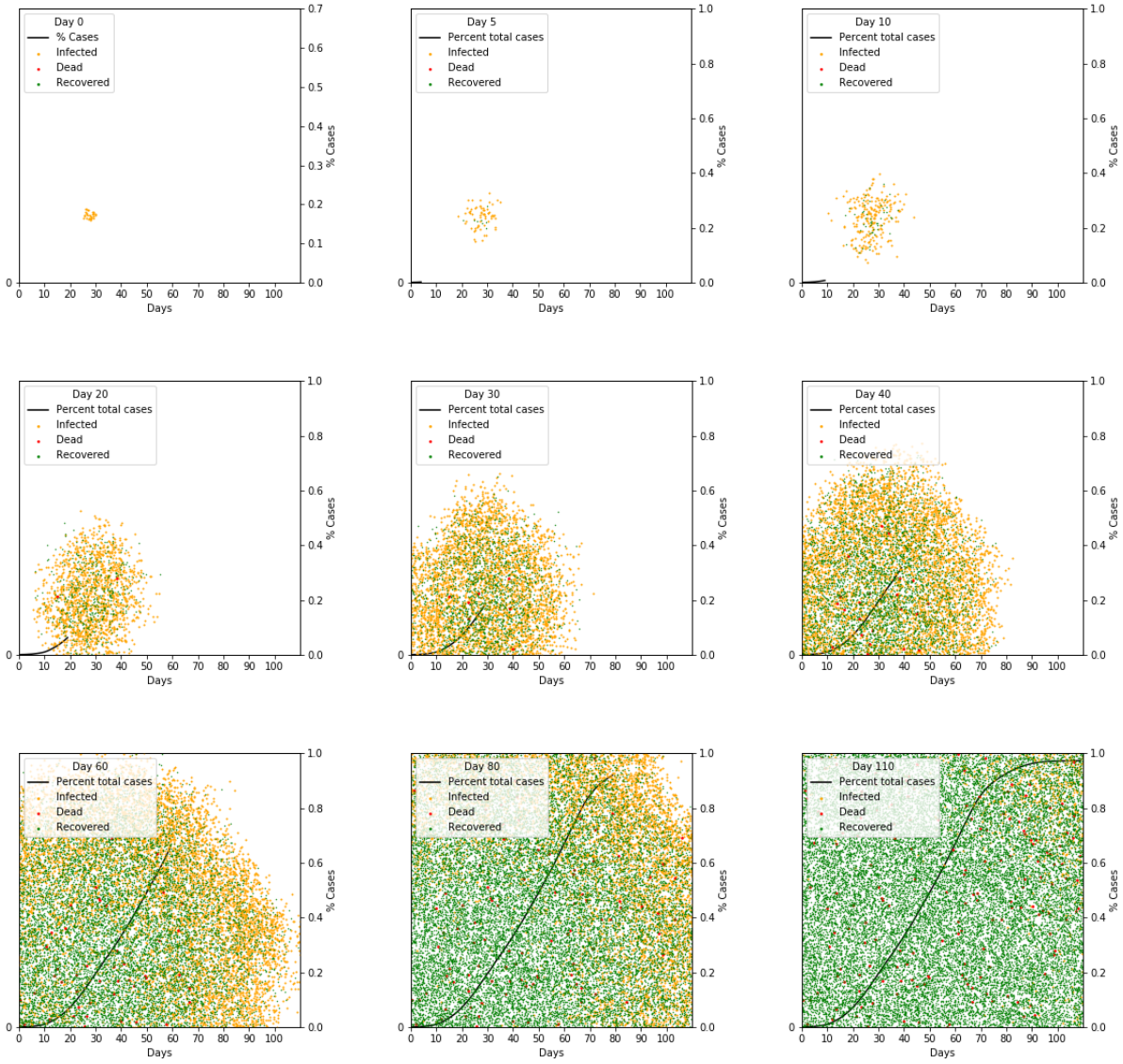

Table 1: Location by time of day

Location type	Period 1	Period 2	Period 3
City	All except sYmptomatics	No-one	No-one
School/Work	No-one	Young except sYmptomatics	No-one
Home	sYmptomatics	sYmptomatics, Not employed, Old	All

stay Home, depending on their demographic and/or health state[12]. A summary of the location visited by agents by time of day is reported in Table 1.

Agents who are symptomatic must stay at home in all three periods. If not symptomatic, all agents visit the City in Period 1, and all Young agents visit the School/Work location in Period 2, when the other agents stay Home.

An agent becomes infected (with some probability) when she is located within a minimum distance from an infected agent (see Appendix B for details on the calibration of these parameters). Movement in the City follows the same rules as in the Spatial-SIR model. Each Young is randomly assigned to a School/Work location. School/Work locations are far from each other (that is, there is no possibility of contagion for agents that belong to different School/Work location). Young agents are randomly placed within their assigned School/Work locations but do not move within them. These locations are denser than the City, with density calibrated according to the parameters described in the next section. Finally, agents are assigned to families located in homes that are far from each others. While at home, agents that belong to the same family share the exact same location.

The distinction we introduce across the three locations (City, School/Work, Home) is meant to abstractly capture different relative densities in agents' social interactions. The School/Work location is meant to represent a non random location that is visited every day by the same set of people, and is denser than the city. Home naturally represents the location with the tightest interactions. Accordingly, we assume that family members share the same position at Home, that is, they are necessarily in contact with each other. At School/Work and in the City, on the other

[12]Agents might be restricted to visit some location also as a policy choice. We discuss these restrictions in the next section.

Figure 2: Dynamics of infections in the Structured Spatial-SIR and locations of infections

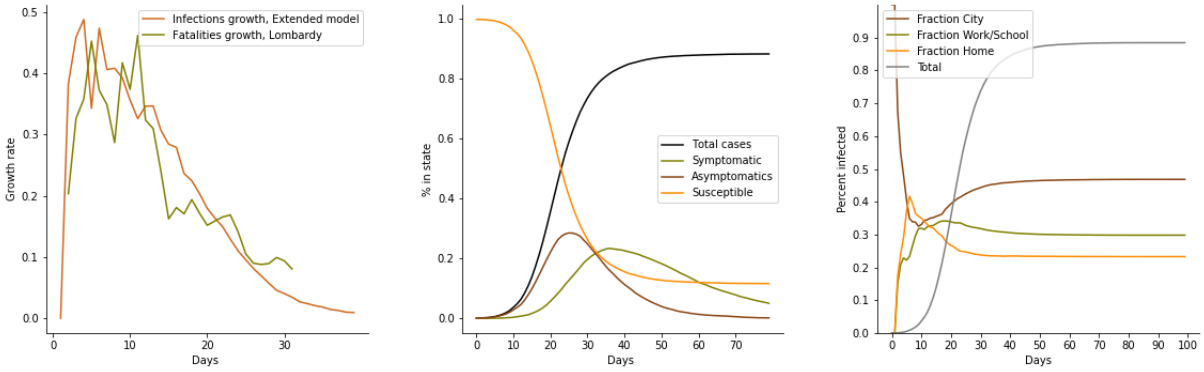

hand, only if people are close they are in contact (as in the SIR in space model, with homogeneous agents).

2.2.1 Age, Occupation, Location of Infection

To calibrate the Structured dimension of the Spatial-SIR we use data from the 2018 American Community Survey (ACS) to classify agents by type and allocate them to households replicating the size and age distribution of American households. We calibrate then relative density of the three locations to match the data on the distribution of contacts reported by Mossong et al. (2008); see Appendix B for details.

Figure 2 shows in the left panel the goodness of fit of our calibration of the Structured Spatial-SIR. Indeed our calibration is able to match well the initial growth rate of the epidemic (proxied, as before, by the growth rates of deaths in Lombardy). The central panel reports the percent of the population in three different states at the steady-state. The right panel shows instead the distribution of infections by location. Table 2 reports summary outcomes by type and location at the end of the infection (the Steady-state).[13] The total fraction of Recovered and Dead in the population at the Steady-state is 0.89; 47% of these individuals have been infected in the City, 29% in the School/Work location, and 23% at Home.

At a fundamental general level, our simulation analysis of the Structured Spatial-SIR model demonstrates that *local* herd immunity - which in Bisin and Moro (2020a) we argued explains the dependence of the dynamics of the epidemic from geographic characteristics - also explains the dependence of the dynamics of the epidemic from location and demographic characteristics. With respect to location, the City originates more infections than School/Work and School/Work more than Home, even

[13]Figures and Tables are obtained averaging over 20 replications.

Table 2: Structured Spatial-SIR: Outcomes

	Infection location			Steady-state outcomes		
	City	W/S	Home	D	R	Peak A+Y
All	0.472	0.294	0.234	0.010	0.876	0.446
Young	0.372	0.427	0.201	0.005	0.933	0.486
Not employed	0.626	0.000	0.374	0.005	0.815	0.383
Old	0.777	0.000	0.223	0.036	0.719	0.365

All figures are fractions of population conditional on type of agent indicated in the first column (averages of 20 random replications). D = Fatalities, R = Recovered, A = Asymptomatics, Y = Symptomatics. Last column: maximum fraction of active cases (symptomatics and asymptomatics) over the entire infection period.

though Home is the most dense location and the City is the least dense. This is because the ranking of the locations in terms of density is opposite to the ranking in terms of size. Herd immunity is achieved *locally* earlier at Home and at School/Work than in the City. The dynamics of the infection by location shows a larger fraction of infections at Home than at School/Work and in the city after about 10 days, when the City relative infection rate starts to pick up.[14]

With respect to the demographic structure the epidemic is more concentrated on the Young because of their exposure to more contacts at School/Work than at Home. The epidemic hits differentially the Old and the Not employed only because of family structure: relative to the Old, the not employed live in households with relatively more young individuals that are infected at School/Work locations. These effects of local herd immunity are akin to a selection effect, whereby the epidemic spreads selectively by location and demographic structure.[15]

2.3 The Behavioral Structured Spatial-SIR

Most epidemiological models employed in forecasting do not formally account for behavioral responses to the epidemic; see e.g., Ferguson et al. (2020) for SARS-CoV-2. In this case, as in our analysis in the previous sections, the number of daily contacts in the population is constant.

In this section we model agents responding to the dynamics of the epidemic by choosing to limit their contacts. Following Keppo et al. (2020), we introduce a reduced-form behavioral response, represented by a function $0 \leq \alpha(I_t) \leq 1$, rep-

[14] The dynamics of the fraction of infections by location at the beginning of the outbreak is driven by the initial condition, which has all the exogenous infected agents at $t = 0$ in the City.

[15] See Gomes et al. (2020) and Britton et al. (2020) for related theoretical analyses

resenting the fraction of agents who are choosing not to interact in the City as a function of the number of infected in the population:[16]

$$\alpha(I_t) = \begin{cases} 1 & if \;\; I_t \leq \underline{I} \\ \left(\frac{\underline{I}}{I_t}\right)^{1-\phi} & if \;\; I_t > \underline{I} \end{cases} . \tag{1}$$

We rank the agents (and School/Work locations) by contagion-risk aversion. Agents choosing not to interact in the City (and School/Firms leaving agents at home) are the most contagion-risk averse. We assume that all agent still have to work during Period 2 if employed. However, in our simulations we assume that some firms and schools adopt behavioral responses similar to the agents', that is, they choose to shut down operations or to allow workers to work remotely, to limit infections at school or work.

Self-Isolating Agents and Schools/Firms Operating Remotely

We calibrate agents' behavioral responses following the estimate $\alpha(I_t)$ obtained by Keppo et al. (2020) using Swine flu data. We calibrate the firms' response from data by Dingel and Neiman (2020) on the share of jobs that can be done remotely; see the Appendix for details. For this calibration we report the effect of the behavioral responses in Figure 3 and Table 3, where we also report some results from Table 2 for ease of comparison. The right panel of Figure 3 shows that at the peak of infections about 14% of individuals are discouraged from visiting the city during Period 1 and 29% are left Home from School/Work in Period 2.

On the left panel we observe that the peak number of active cases, once accounting for the behavioral response of agents and firms, is 13 percentage point lower (from 45 to 32 percent of the population). At steady state, this difference persist to generate a total number of Recovered and Dead equal to 77 percent of the population versus 89 with no behavioral response.

[16] In Spatial-SIR with state space (S, A, Y, R, D), the behavioral response will depend on A. Since the fraction of asymptomatics is not observable, behavioral response could only depend on the number of symptomatics, as a proxy; with Rational Expectations, however, the agents know (rationally infer) the equilibrium map from Y to A, say $A(Y)$, possibly with noise; see Bisin and Moro (2020b) or Gans (2020).

Figure 3: Calibrated behavioral responses in the Behavioral Structured Spatial-SIR

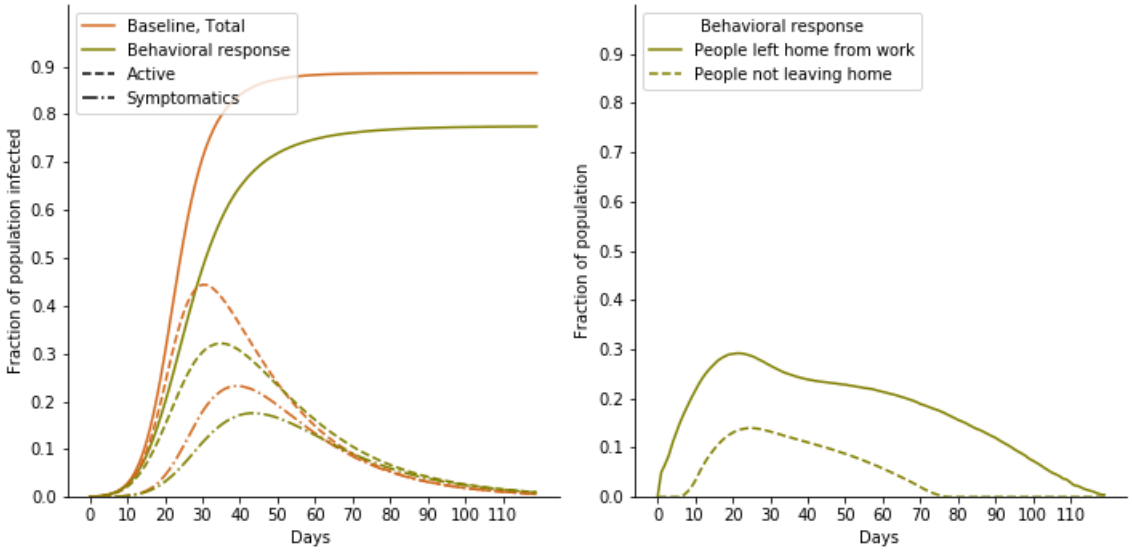

Several interesting effects of the behavioral response of agents and firms can be seen disaggregating outcomes by location of infection and demographic structure (see Table 3). First, the fraction of infections occurring at Home is almost 10 percentage points higher with behavioral response. The simmetric opposite effect is mostly concentrated at School/Work rather than in the City, whose fractions of infection decrease, respectively, of 9 and 1 percenteage points. The total reduction of infections at School/Work affects mostly the Young, who get infected more at Home (from 20 to 31 percent) and less at School/Work (from 43 to 30 percent). At the steady-state, the proportion of Young Recovered or Dead decreases fro 94% to 82%.

The most important implication resulting from this simulation are the indirect effects of the behavioral response across locations and demographic types. Specifically, the behavioral responses of (mostly) the Young, (mostly) in the School/Work location have a sizable important effect on the Old in the City (the Old get infected mostly in the City, over 70%, with or without behavioral response). Most importantly, the compensating effect of higher infections at Home with behavioral response is of reduced importance for the Old because of family composition (the Old tend to live with other Old). At the steady-state, the proportion of Old Recovered or Dead decreases from 73% to 63%.[17] The effect of behavioral response on the Not employed

[17] A simulation - which we do not report in the text - where we only allow for a behavioral response by firms, has a much smaller effect on the Old, suggesting that the main effect on the Old goes through the reduction of infections in the City.

Table 3: Behavioral Structured Spatial-SIR: Outcomes

	Initial location			Steady-state outcomes		
	City	W/S	Home	D	R	Peak A+Y
All	0.463	0.205	0.332	0.008	0.766	0.323
All (no behavior)	0.472	0.294	0.234	0.010	0.876	0.446
Young	0.394	0.296	0.309	0.004	0.819	0.349
Not employed	0.537	0.000	0.463	0.004	0.728	0.290
Old	0.726	0.000	0.274	0.029	0.599	0.249

No behavior (second row): data from the model with no behavioral response, Table 2. All figures are fractions of population conditional on type of agent indicated in the first column (averages of 20 random replications). D = Fatalities, R = Recovered, A = Asymptomatics, Y = Symptomatics. Last column: maximum fraction of active cases (symptomatics and asymptomatics) over the entire infection period.

is instead moderated, relatively to the Old because their family composition induces them to be infected more at Home.

3 Lockdown policies

In this section we explore the effects of various policies similar to non-pharmaceutical interventions proposed and implemented by various administrations during the COVID-19 outbreak. Our goal is to exploit the spatial nature of the model, the structure of the network of interactions and the (distinction by) demographic characteristics of the agents to analyze the different impact of these policies both in the aggregate and across types.

We first study a general lockdown, that is, (i) a City lockdown that requires individuals to stay home in Period 1 if the fraction of actively infected (Asymptomatics plus sYmptomatics, $A + Y$) is above a given threshold; and (ii) A School/Work lockdown that requires 50 percent of firms to shut-down so that 50 percent of workers/students (work/study remotely and hence) stay home during Period 2 if the fraction of Asymptomatics plus sYmptomatics is above a given threhsold.[18] For this form of a general lockdown we present simulations for the dynamics of infection distinguishing different thereshold for imposing the lockdown and different reopening

[18]The choice of using the fraction of Asymptomatics plus sYmptomatics as a threshold is without loss of generality if we assume that policy makers with perfect foresight can infer the fraction of actively infected agents in the population from the random testing a sample of the population. In practice, foresight is limited and testing strategies are often biased, and it is hard to quantify both the sign and magnitude of the bias.

policies. We then study two selective lockdown policies, the first in which only the City is locked down (workers/students are allowed to visit the Work/Study location) and the second in which the Old are confined to live at Home or in quarantine facilities of different sizes.

In all the cases we study, policies overlap with the behavioral response; that is, they are applied to the population of agents and firms randomly, not accounting for their behavioral response. In other word, lock-down policies may apply to agents (resp. firms) that would have chosen to self-isolate (resp. shut down) even in the absence of the policy.[19]

3.1 A general lockdown of the city and workplace

We study the effects of a generalized lockdown of the City and 50 percent of Work/-School locations. We consider policies where the lockdown is applied when the fraction of active cases, $A + Y$, reaches a given fraction of the population. We reports results regarding different policies regarding when to reopen the City and the School/Work locations operating remotely. The results reveal the trade-off between flattening the curve of active cases and delaying the reaching of global herd immunity.

3.1.1 Reopen forever after active cases return to the fraction which triggered the lockdown

We start by studying the case in which both City and School/Work reopen forever after active cases return to the fraction which triggered the lockdown (10, 5, and 3.5 percent). In this case, because the lockdown may have delayed the population reaching herd immunity, infections may increase again after reopening.

[19]This can be interpreted as a first example of application of Lucas Critique argument in this context; see Section 4 for a more articulated discussion and interesting examples.

Figure 4: Lockdown and reopen forever

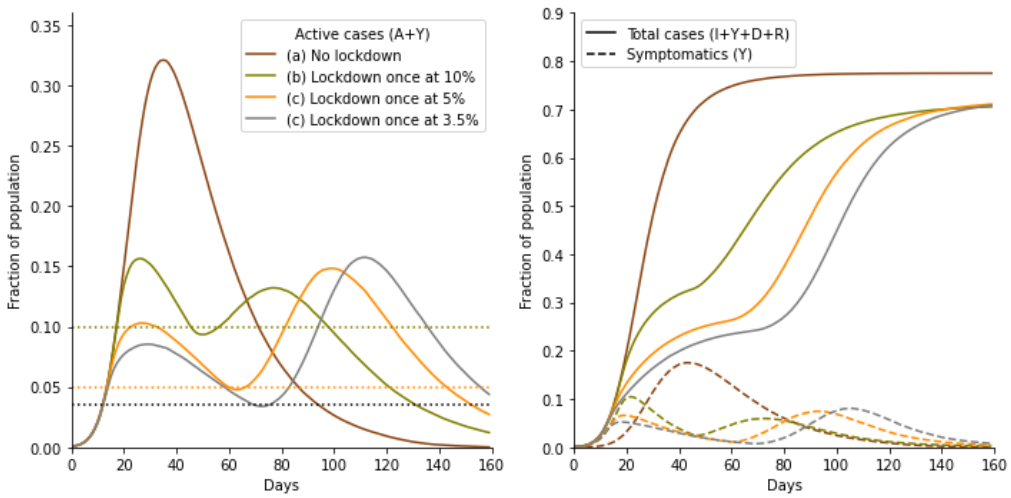

Table 4: Lockdown and reopen forever

	Infection location			Steady-state outcomes		
	City	W/S	Home	D	R	Peak A+Y
3.5 percent lockdown rule						
All	0.363	0.233	0.404	0.007	0.715	0.159
Young	0.292	0.330	0.378	0.004	0.779	0.163
Not employed	0.436	0.000	0.564	0.003	0.669	0.153
Old	0.671	0.000	0.329	0.025	0.514	0.144
5 percent lockdown rule						
All	0.362	0.231	0.407	0.007	0.712	0.150
Young	0.292	0.327	0.381	0.004	0.777	0.155
Not employed	0.434	0.000	0.566	0.004	0.663	0.141
Old	0.668	0.000	0.332	0.025	0.508	0.134
10 percent lockdown rule						
All	0.363	0.225	0.412	0.007	0.703	0.158
Young	0.296	0.318	0.386	0.004	0.769	0.183
Not employed	0.430	0.000	0.570	0.003	0.658	0.129
Old	0.661	0.000	0.339	0.024	0.492	0.112
15 No lockdown						
All	0.463	0.205	0.332	0.008	0.766	0.323

Lockown of the City and of 50 percent of the School/Work locations. No lockdown: results the behavioral model with no lockdown, Table 3. All figures are fractions of population conditional on type of agent indicated in the first column (averages of 20 random replications). D = Fatalities, R = Recovered, A = Asymptomatics, Y = Symptomatics. Last column: maximum fraction of active cases (symptomatics and asymptomatics) over the entire infection period.

The results are displayed in Figure 4 and Table 4. We notice that the flattening of the infection curve is substantial. In all cases the peak of active cases with lockdown is less than half than without. The reduction of Dead and Recovered at the steady-state is substantial. Importantly, the lockdown has rather large effects on the Old. Comparing Table 4 with Table 3, in fact, reveals that the fraction of Dead and Recovered decreases under all policies by about 10 percentage points for the Old and only about half as much for the Young (and Not employed). While either lockdown reduces the fraction of Dead at steady-state of only one tenth of 1 percent, this reduction is four to five times as big for the Old.

Importantly, the lockdown strategy interacts in rather subtle ways with the dynamics of herd immunity. When the lockdown is placed too early (5 percent in our simulation), the fraction of infected is too small, herd immunity is too far out, and at reopening a second wave of infections reaches a peak higher than the first one.

3.1.2 Intermittent reopening until active cases are stably declining

We study now the case in which, when active cases return to the fraction which triggered the lockdown (5 and 10 percent), a period of intermittent reopening and lockdown is imposed so as to avoid a second wave of infections. Results are reported in Figure 5 and Table 5. Interestingly, the lenght of the intermittent reopening and lockdown period is about inversely related to the threshold (18 days for 10 percent lockdown and 58 days for 5 percent) because herd immunity is delayed by an early lockdown. The total Dead and Recovered is about 3 percentage point lower when the second wave is avoided than when it is not.

Figure 5: Lockdown and reopen when stably declining

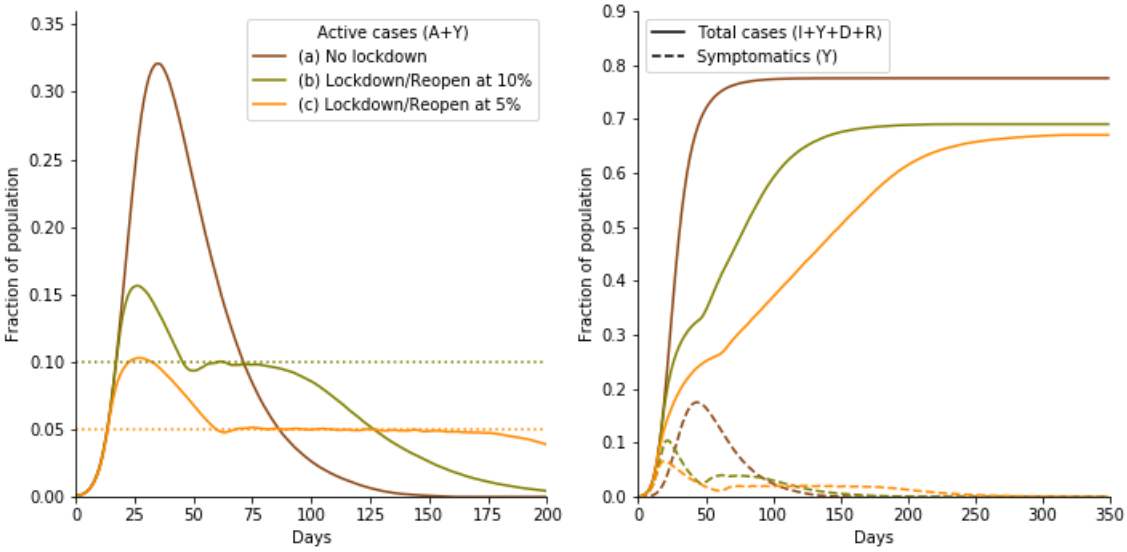

Table 5: Lockdown and reopen when stably declining

	Infection location			Steady-state outcomes		
	City	W/S	Home	D	R	Peak A+Y
10 percent permanent lockdown						
All	0.342	0.228	0.429	0.007	0.684	0.158
Young	0.278	0.320	0.402	0.004	0.752	0.183
Not employed	0.405	0.000	0.595	0.003	0.635	0.129
Old	0.646	0.000	0.354	0.023	0.468	0.086
5 percent permanent lockdown						
All	0.306	0.242	0.453	0.007	0.665	0.104
Young	0.242	0.336	0.422	0.004	0.738	0.125
Not employed	0.368	0.000	0.632	0.003	0.612	0.080
Old	0.622	0.000	0.378	0.021	0.435	0.050

All figures are fractions of population conditional on type of agent indicated in the first column (averages of 20 random replications). D = Fatalities, R = Recovered, A = Asymptomatics, Y = Symptomatics. Last column: maximum fraction of active cases (symptomatics and asymptomatics) over the entire infection period.

3.1.3 Cautious reopening

Finally, we study several cases in which reopening is more cautiously set: a 5 percent reopening threshold for the 10 percent lockdown and a 2 percent reopening threshold for the 5 percent lockdown. This is an interesting health policy strategy because, as we have seen in the previous sections, the lockdown strategy interacts with the dynamics of herd immunity and an early reopening can induce an high second wave of infections.

Results are in Figure 6 and Table 6. With respect to the case in which reopening occurs at the same threshold as the lockdown, in this case herd behavior is more advanced at reopening and the second wave is substantially dampened. The peaks of the second wave occur at about 8% as opposed to 13% of the population, for the 10 percent lockdown. The result is even more striking for the 5 percent lockdown. In this case, with reopening at 5 percent, the second wave was higher then the first (15 [percent). With cautious reopening at 2 percent, instead, the second wave is dampened to 5 percent. Interestingly, hovever this triggers another lockdown and hence a third wave whose peak is below 5 percent. Relatedly, the fraction of Dead and Recovered at steady-state is lower with cautious reopening, about 3 and 8 percentage points, respectively, for the 10 and the 5 percent lockdowns. Cautious reopening, we conclude, is particularly effective for the 5 percent lockdown, where reopening at 5 percent induced a large second wave and a fraction of Dead and Recovered at steady-state larger than with a less restrive lockdown at 10 percent (with reopeniong at 10 percent).

Figure 6: Lockdown and cautious reopening

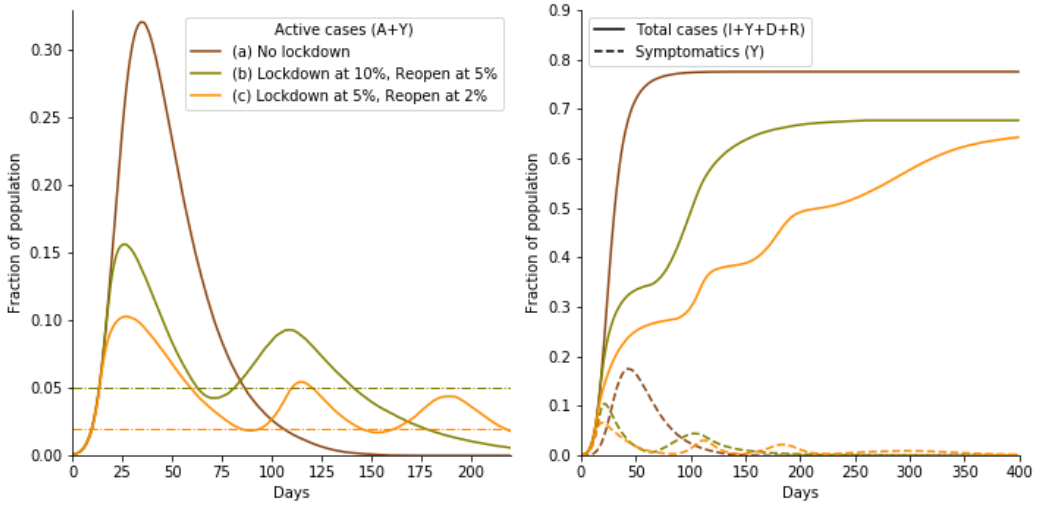

Table 6: Lockdown and cautious reopening

	Infection location			Steady-state outcomes		
	City	W/S	Home	D	R	Peak A+Y
5 percent lockdown - 2 percent reopening						
All	0.292	0.254	0.453	0.006	0.630	0.104
Young	0.230	0.351	0.419	0.004	0.706	0.125
Not employed	0.358	0.000	0.642	0.003	0.570	0.080
Old	0.609	0.000	0.391	0.019	0.397	0.050
10 percent lockdown - 5 percent reopening						
All	0.339	0.235	0.426	0.007	0.674	0.158
Young	0.273	0.329	0.398	0.004	0.743	0.183
Not employed	0.408	0.000	0.592	0.003	0.622	0.129
Old	0.646	0.000	0.354	0.022	0.457	0.086

3.2 Selective Lockdowns

In this section we study two selective lockdown policies. In the first one, we limit the lockdown to the City and we let firms/school decide whether to operate remotely. In the second one, we limit the lockdown to the Old, a policy aiming at reducing total fatalities while bearing limited economic costs (the Old are not economically active, but suffer a higher fatality rate than other demographic groups). Both these lockdown policies have the important property that they are much less costly, economically, as worker/students remain active. This consideration need to be traded-off with additional costs in terms of health outcomes at the steady-state or at the peak, e.g., if the society has a constraint with respect to health care resources like hospital/ICU beds. Furthemore, while these selective lockdowns have positive direct effects in terms of economic costs, indirect effects across locations and/or demographic types could in priciple substantially limit their advantage over general lockdowns.

3.2.1 City-Only lockdown

Results for the City-Only lockdown are reported in Figure 7 and Table 7, with respect to a 10 percent lockdown with cautious reopening at 5 percent. Interestingly, in this case, with respect to the general lockdown, the first peak in $A + Y$ is higher (18.6

Figure 7: City-Only lockdown

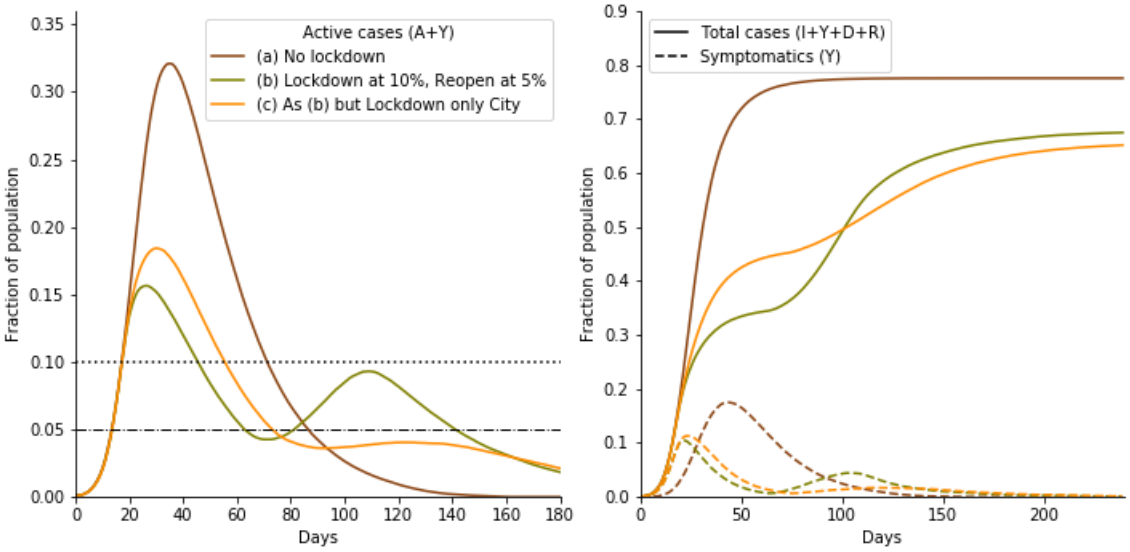

percent rather than 15.8), but there is no significant second wave. Furthermore, the total fraction of Dead and Recovered at the steady-state is 2 percentage points lower. This is striking, as the City-Only lockdown is much less costly, economically, than the general lockdown. According to these simulations, the City-Only lockdown has extra health costs only inasmuchas the first wave might be too high with respect to a possible constraint in terms of health care resources. In other words, indirect effects, e.g. from City to Home, do not appear to limit the advantages of the City-Only lockdown in our simulations.[20]

3.2.2 Old-Only lockdown

Results for the Old-Only lockdown are reported in Figure 8 and Table 8, with respect to a 5 percent lockdown with a period of intermittent reopening and lockdown at 5 percent to avoid a second wave of infections. Comparing it with the case in which the lockdown is general (that is includes the Young and the Not Employed as well), it is remarkable that the number of stationary Dead between the Old is more than halved, from over 2 percent to less that 1 percent. The peak of active cases remains rather high, as the Young and the Not Employed keep interacting in the City and the Young also at School/Work. This high peak does not necessarily affect possible constraints on health care resources if the Old use them relatively more intensely.

[20] As we repeatedly noted, we do not aspire to quantitatively precise prediction because the calibrated model we simulate is very stylized.

Table 7: City-Only lockdown

	Infection location			Steady-state outcomes		
	City	W/S	Home	D	R	Peak A+Y
City-Only lockdown, at 10 percent, reopening at 5 percent						
All	0.264	0.296	0.440	0.006	0.650	0.186
Young	0.201	0.403	0.396	0.004	0.738	0.225
Not employed	0.336	0.000	0.664	0.003	0.574	0.138
Old	0.600	0.000	0.400	0.018	0.387	0.086
General lockdown						
All	0.339	0.235	0.426	0.007	0.674	0.158

As for the City-Only lockdown, our simulations of the Old-Only lockdown, suggest that indirect effects, e.g., from Young to Old or from School/Work to Home, do not substantially limit its advantage.

The simulations we have just reported refer to the case in which the Old are locked-down at Home, where they interact with Young and Not Employed agents. In Figure 9 we report $D + R$ (left panel) and D (right panel) at steady-state for different simulations where the Old are locked-down in nursing homes of different sizes (the dot is the case where the Old are locked-down at their Home). It is noteworthy that the number of Dead increases steeply with the size of the nursing homes, reaching 2 percent for homes with 50-agents each. It is also interesting the lockdown of the Old at Home is equivalent in terms of infection and fatality rates to one where the Old are locked-down in nursing home of about size 10. This is a consequence of the indirect interactions across location hurting the more susceptible demographic group.

Figure 8: Old-Only lockdown

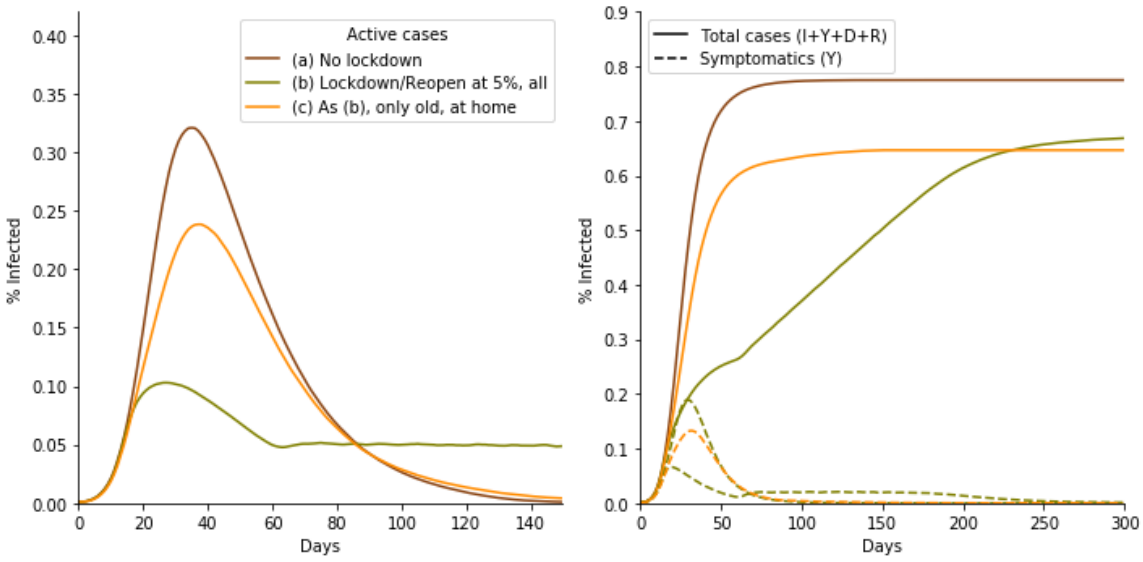

Table 8: Old-Only v. General lockdown

	Infection location			Steady-state outcomes		
	City	W/S	Home	D	R	Peak A+Y
All (Old-Only)	0.440	0.151	0.410	0.005	0.645	0.240
All (General)	0.306	0.242	0.453	0.007	0.665	0.104
Young (Old-Only)	0.427	0.200	0.372	0.004	0.748	0.282
Not employed (O-O)	0.522	0.000	0.478	0.003	0.686	0.246
Old (Old-Only)	0.303	0.000	0.697	0.009	0.192	0.052
Old (General)	0.622	0.000	0.378	0.021	0.435	0.050

Figure 9: Size of nursing homes

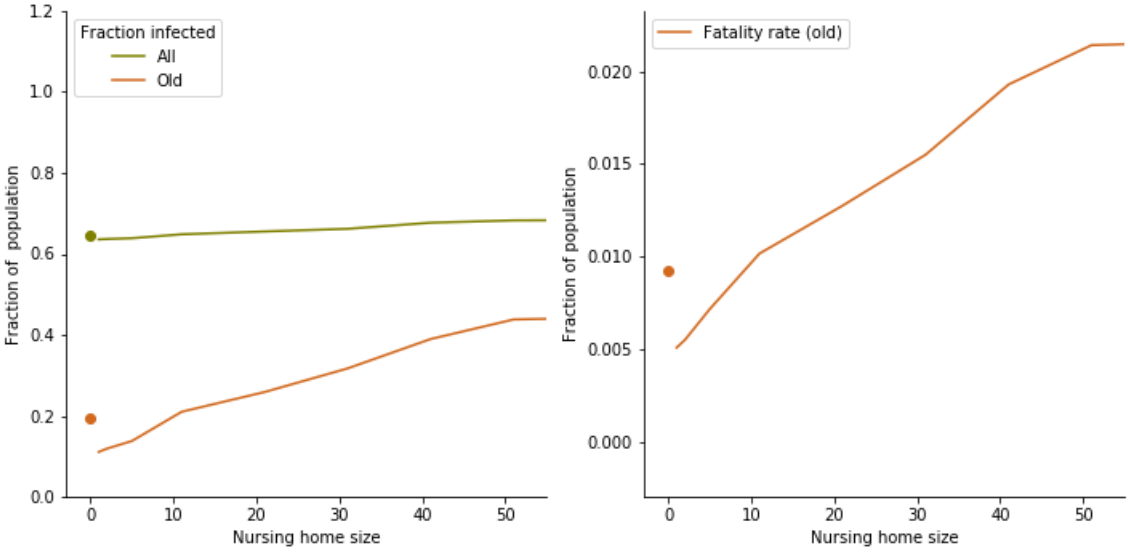

Note: the dots corresponding to the nursing home size equal to zero report simulations where the Old are isolated at home.

4 An Exercise in the Lucas Critique

In this section we illustrate the implications of what economists refer to as the *Lucas Critique*, in the context of epidemiological models.[21] We have already shown, in the previous section, that the behavioral response of agents and firms to the dynamics of an epidemic is bound to have important effects on the dynamics themselves. We now discuss how policy evaluations and interventions disregarding that agents' and firms' "decision rules vary systematically with changes in the structure of series relevant to the decision maker" might lead to policy decisions that are very costly in terms of their effects on the dynamics of the epidemic.

4.1 Policy maker error

In this section we simulate the prediction error of a policy maker evaluating different lockdown policies while not anticipating the behavioral response of agents and firms

[21] From Lucas (1976). In its original formulation, the Critique is summarized as follows:

> "Given that the structure of an econometric model consists of optimal decision rules of economic agents, and that optimal decision rules vary systematically with changes in the structure of series relevant to the decision maker, it follows that any change in policy will systematically alter the structure of econometric models."

Figure 10: Counterfactual: Policy maker error - lockdown at 10%, reopen at 5%

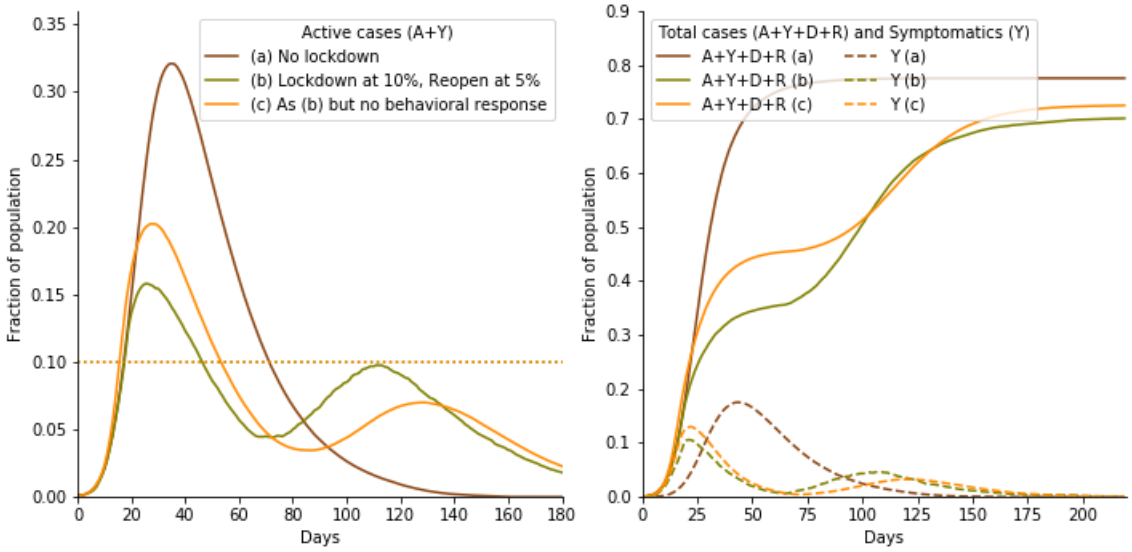

to the dynamics of the epidemic. We interpret the dynamics without behavioral response as the policy maker's prediction of the effect of the lockdown and the case with response as the actual outcome of the lockdown.

We report the case of a lockdown at 10 percent with reopening at 5 and a lockdown at 5 percent with reopening at 2; respectively in Figure 10 and 11 (we do not report tables for these simulations). In both cases, the policy maker predics a higher peak than it actually occurs. On the other hand he/she will face an earlier and higher than predicted second wave.

4.2 Policy maker error when re-calibrating the reopening policy

In this section we postulate a more articulate procedure to evaluate different lockdown policies on the part of a policy maker who does not anticipate the behavioral response of agents and firms. Consider a policy maker who evaluates lockdown interventions assuming no behavioral responses, but chooses the reopening threshold as a consequence of a policy re-valuation after the lock-down, still disregarding the behavioral response. More specifically, consider the case where, at the re-evaluation stage, the policy maker naively attributes the lower-than-predicted peak of infections to the effect of fewer people visiting the City and School/Work locations, generating lower contact rates and slower diffusion of the epidemics. The policy maker, however, continues to disregard the fact that behavioral responses are a function

Figure 11: Counterfactual: Policy maker error - lockdown at 5%, reopen at 2%

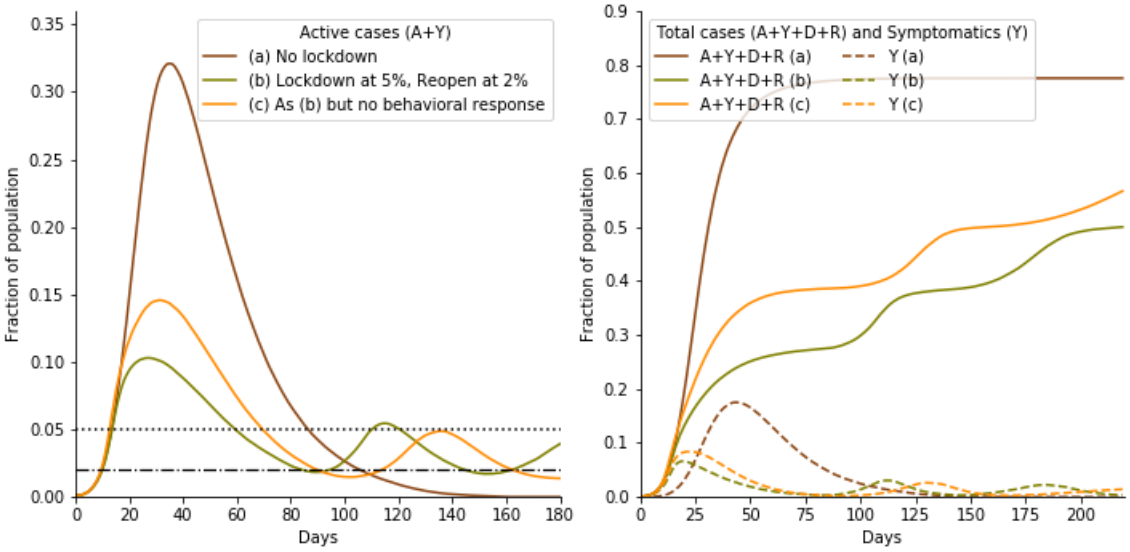

of the number of cases, and re-evaluates the reopening policy assuming that people visiting the City and School/Work locations remain at the (lower) level observed at the re-evaluation.

The adverse effects and the costs of this procedure, are clearly seen in the case in which a policy maker sets up a 3.5 percent lockdown rule with the goal of not experiencing a peak active cases over about 13 percent, as predicted by the model without behavioral response (see Figure 12). When reaching the peak, which occurs at about 8 percent, the policy maker re-evaluates its reopening policy, re-calibrates its model and computes a new reopening rule. The re-calibration and the new reopening rule are computed postulating still no behavioral response upon reopening. In our simulations, we run the model to find the reopening rule that would generate 13 percent active cases at the peak in the policy maker's re-calibrated model.

The error induced by the policy maker recalibrating the reopening policy is clearly apparent in the Figure. Since there is not enough herd immunity at the first peak, the policy-maker delays reopening until the fraction of active cases is about 1 percent. Nonetheless the recalibration misses the behavioral response of agents and firms, who increase the contact rate in both the City and the Work/School due to the low infection rates. As a consequence, the second wave is much higher than the first and ends up actually reaching a peak of about 15 percent, substantially higher than the government original target of 13 percent. Considering that the lock-down and

Figure 12: Counterfactual: Lockdown at 3.5% with re-calibrated reopening

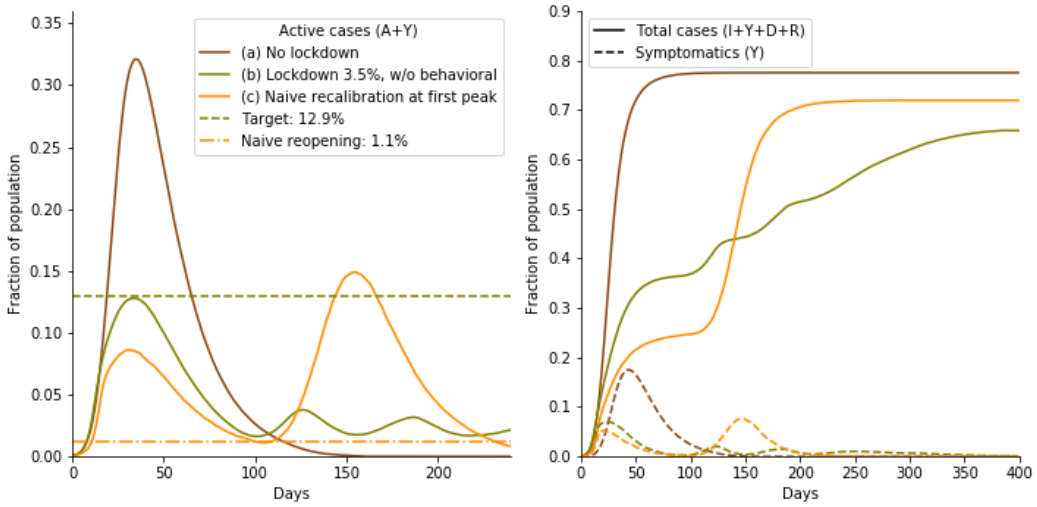

Notes: (a): Results from the simulation with behavioral responses, Section 2.3. (b): Results from the model with no behavioral reaponses, with a lockdown threshold policy at 3.5% with a target peak at 12.9% (c): Results from adjusting the reopening policy at 1.1% after the first peak.

opening threshold are calibrated to flatten the curve of the infections so has to avoid hitting a constraint on the available health care resources, this simulation implies that health care resources will be under-utilized after lock-down (that is, the lock-down will turn out to be stricter than necessary) and they will instead be over-run after reopening, with potentially high human costs.

Interestingly, the costs associated to this policy making procedure disregarding behavioral responses are less apparent in the case of a lockdown at 5 percent so as to avoid a peak higher than about 15 percent of active cases (see Figure 13). It is still the case that the policy maker, after observing a smaller than expected first peak, expects the a low infection rate for the future, induced by (what she expects to be a constantly) lower contact rate. She then decides to reopen too soon, when cases are low and hence the behavioral response of agents and firms increases the contact rate. As a consequence, the epidemic picks up giving rise an unexpected second wave of the infection as agents and firm. However, in this case the second peak after recalibration is higher than the first, but near the 15 percent target, not higher as in the previous case. Interestingly, what happens in this case is that, while the recalibration misses the behavioral response leading agents and firms increase the contact rate after the first peak, it also misses the herd immunity generated by this behavior. The effect of herd immunity is larger both because initial lockdown

Figure 13: Counterfactual: Lockdown at 5% with re-calibrated reopening

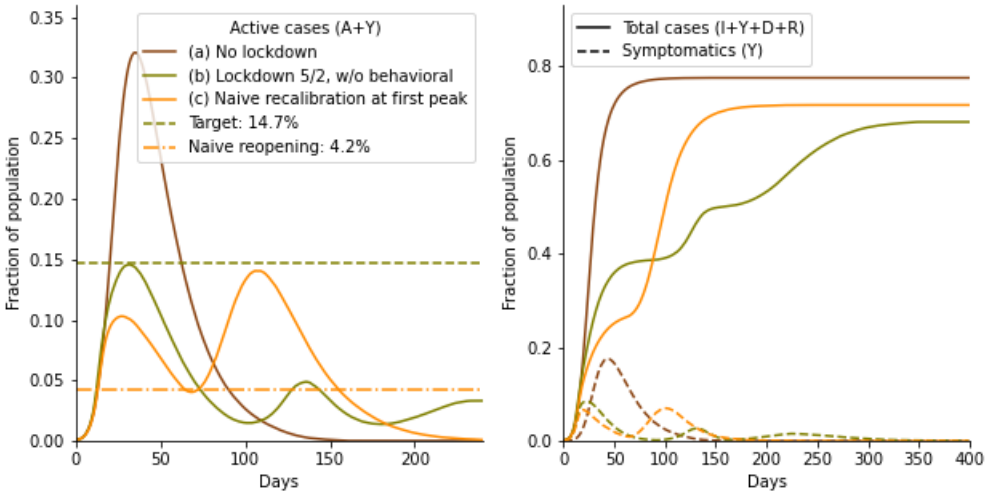

Notes: (a): Results from the simulation with behavioral responses, Section 2.3. (b): Results from the model with no behavioral reaponses, with a lockdown threshold policy at 5% with a target peak at 14.7% (c): Results from adjusting the reopening policy at 4.2% after the first peak.

is set at 5 percent than at 3.5 percent, because of the relatively higher firstpeak of infections, and because, after the government re-evaluation, when active cases are declining, more people than the government expect visits the city and gets infected.

5 Conclusions

In this paper we developed a parsimonious stylized model which, in our objectives, represents the epidemiological component of a more general economic model in which the policy trade-off between economic activity and epidemic diffusion is evaluated. The model is designed to qualitatively and quantitatively identify the role of the interactions between several fundamental "forces" driving the dynamics of an epidemic, like (global and local) herd immunity, network and demographic heterogeneity, behavioral responses of agents and firms to infections, and Non-Pharmaceutical Policy interventions. In this respect we stress that the role of Lucas Critique arguments, which identify the adverse effects and the costs of policy interventions disregarding behavioral responses, is potentially first order, qualitatively and quantitatively (dependending on the calibration).

A Appendix: Theoretical Structure of SIR and Spatial-SIR

We refer to Appendix A in Bisin and Moro (2020a) for a formalization of the Spatial-SIR we extend in this paper. The extension we adopt in this paper adds demographic and network structure as described, but does not alter the mechanics of the epidemic state transitions.

B Appendix: Calibration

We calibrate the parameters of Spatial-SIR to the dynamics of the SARS-CoV-2 epidemic.[22] The parameters we choose in the calibration of the aggregate model are summarily reported in Table 9.

Geography

The City is a square of area equal to 1. People are located in the City by randomly drawing their x and y coordinates indipendently from a Uniform distribution $\sim U[0,1]$. At all $t > 0$, individuals are relocated at distance μ from their location at $t-1$, in a direction drawn randomly from a Uniform distribution $\sim U[0, 2\pi]$. School/Work locations are are squares of size calibrated as described below. All School/Work locations are far from each other and far from the city in order to prevent contagion between people belonging to different schools/workplaces. The location of individuals within School/Work locations is randomly drawn as in the City, but does not change over time. Homes have no dimension and are far from both School/Work locations and from the city.

Agent types and family composition

We use data from the 2018 American Community Survey (ACS) to classify agents by type and allocate them to households replicating the size and age distribution of American households. Specifically, we calculate from the ACS the distribution of family compositions by Young/Old age of respondents not leaving in Group Quarters, and construct households of sizes and Young/Old compositions replicating this distribution. The age cutoff for being classified as Old is 65. We then create households of size 50 containing either only Young or only Old individuals to replicate the fraction of Young and Old ACS respondents living in group quarters (2.9% of Old

[22] We acknowledge the substantial uncertainty in the literature with respect to even the main epidemiological parameters pertaining to this epidemic. As we noted in the introduction, this is less problematic when aiming at understanding mechanisms and orders-of-magnitude rather than at precise forecasts.

and 2.4% of Young). In the 2018 ACS, approximately 16 percent of individuals are above 65 years of age. We divide the remaining population to reflect the proportion of the population that are young and either employed or in school, 65 percent, and define the rest, 19 percent, as Not employed. We randomly assign all Young to a number of School/Work locations such that their average size is 100 individuals.

Locations density.

We calibrate the relative density of the three locations to match the data on the distribution of contacts reported by Mossong et al. (2008).[23] In this data, on average, people make 13.5 contacts per day. Furthermore the total number of contacts is distributed as follows: 34% at work or at school, 34% in other locations besides home.[24] Assuming that interactions at home necessarily induce contacts between family members, and with an average family size of 3.3 from the ACS data, this implies 2.3 contacts at home.[25] Of the remaining 11.2 contacts, according to the data in Mossong et al. (2008), about half occur at Work and School and half in what we have categorized as the City. Because a fraction of the population is structurally restricted not to visit the School/Work location (the Old and the Not employed), we need to rescale the number of contacts per day in each location. In the ACS this fraction is 15% and therefore we calibrate that a young and occupied agent (a schoolchild or a worker) receives 17.6 percent (100/85%) more contacts that anyone in other locations. We allocate therefore the 11.2 contacts per day not occurring at home proportionally, 6 at School/Work and 5.2 in the city. We therefore calibrate the contagion radius to match 5.2 contacts on average in the city, given its population. We keep the same contagion radius in the School/Work locations, but calibrate the size of such locations so as to generate 6 contacts, on average.[26]

Initial conditions

At time $t = 0$ we set 30 individuals in Asymptomatic state; all others are Susceptibles. the Asymptomatics at $t = 0$ are those initially located in a position closest to City location $[x = 0.25, y = 0.25]$. We assume they have been infected in the City.

[23] They survey mixing patterns on a sample of the population in eight European countries. We do not exploit cross-country heterogeneity in this section and consider averages.

[24] We ignore the 7 percent of contacts occurring in "multiple" locations.

[25] This is lower than implied by Mossong et al. (2008), but it's an upper bound for the size distribution of families form ACS we use.

[26] With a population of 26,600 individuals on a square of unit side, the contagion radius we obtain is 0.00805. With 100 agents at each School/Work location on a square, the side we obtain is 0.0547.

Table 9: Parameters Values in the Calibration

Parameter	Value
# or people	26,600
family size and group quarters composition	match 2018 ACS
School/Work location average population	100 individuals
group quarter size	50 individuals
School/Work location side	0.003304[28]
mean distance traveled in City	0.028175
contagion radius	0.00805
initially infected	30
prob. of recovery	0.05
prob. of becoming symptomatic	0.09
fatality rate (Old)	0.00533
fatality rate (Young and Not employed)	0.000533
contagion probability (City, School/Work)	0.032
contagion probability (Home[29])	0.064

Infection and contact rates

We calibrate the contagion rate π and the mean travel distance μ to match the daily growth rates of the dynamics of infections, g_t, observed in the first 35 days of epidemics in Lombardy, Italy; see Figure 2, left panel.[27] We assume that that contagion rates are twice as large at Home locations than elsewhere, and that Symptomatic individuals remain contagious at home, but are not contagious elsewhere.

We calibrate the daily fatality rates by type imposing that the Old have 10 times higher fatality rates than the Young and scale their average so that the aggregate infection fatality rate (IFR) is 1%, consistently with e.g., Ferguson et al. (2020).

Transitions away and between the infected states, A, Y, D, R.

The probability to transition away from the Asymptomatic state A, is $\rho + \nu$. We assumed agents are infective only in state A (we assumed that all sYmptomatic

[27] Since the number of infections is not observed, we match the growth rates of infection in the model with the growth rate of deaths in the data. This is justified when, as we assumed, the case fatality rate is aonstant and Death follows infection after a constant lag on average.

[28] Equivalent to 14.2% higher population density than in City

[29] Symptomatics are infective at home with the same probability

agents reduce to zero social contacts). The average time an agents stays in state A is then $T_{inf} = \frac{1}{\rho+\nu}$. We set $\rho+\nu$ to match a theoretical moment which holds exactly at the initial condition in the basic SIR model. Recall R_0 denotes the number of agents a single infected agent at $t = 0$ infects, on average. Let g_0 denote the growth rate of the number of infected agents at $t = 0$. Then, in SIR,

$$\frac{(\mathcal{R}_0 - 1)}{T_{inf}} = g_0. \tag{2}$$

For the current SARS-CoV-2 epidemics, R_0 is reasonably estimated between 2.5 and 3.5.[30] The daily rate of growth of the infection g is estimated = .35 by Kaplan et al. (2020).[31] This implies, from Equation (2), that T_{inf} is between 4 and 7 days (respectively for $\mathcal{R}_0$ between 2.5 and 3.5). Ferguson et al. (2020) use 6.5 days. We set $\rho+\nu = .14$, so that $T_{inf} = \frac{1}{\rho+\nu} = 7$.[32] Furthermore, the average time from infection to death or recovery is reasonably estimated to be 20 days; see e.g., Ferguson et al. (2020). Therefore we set $\rho = .05$ so that $1\rho = 20$. This implies $\nu = .09$.

The case fatality rate, the probabilty of death if infected, is estimated between .005 and .01; see e.g., Ferguson et al. (2020). Since agents remain sYmptomatic in the model, before Recovering, on average $\frac{1}{\nu} = 11$ days, we set the probability of Death for a sYmptomatic, δ, to be 0.001.[33]

Behavioral responses

We set $\phi = 0.88$ as estimated by Keppo et al. (2020) using Swine flu data, and assume people start responding to the spread of the contagion very soon by setting $\underline{I} = 0.01$. The fraction of firms that choose to let workers work remotely is calibrated using the same functional form (eqn. 1). We use the same calibration for $\phi = 0.88$, but we calibrate $\underline{I}$ so that the fraction of school/workplaces that choose to shut down is 50% when the fraction of Asymptomatics is 20% (close to the peak of the Asymptomatics curve in most of our simulations[34]). We believe 50% to be a reasonable guess for the peak given that 24 percent of the population is reported by the 2018 ACS being in schook and that Alon et al. (2020) compute from ATUS data that about 25% of workers work in highly telecommutable jobs; see also Dingel and Neiman (2020), who report that the share of jobs that can be done at home goes from 50% to 30%, across metropolitan areas in the U.S.

[30] For details, see Footnote 32 in Bisin and Moro (2020a)

[31] Alvarez et al. (2020) have .2; Ferguson et al. (2020) have 0.15.

[32] We thank Gianluca Violante for suggesting this calibration strategy.

[33] We assume fatalities cannot occur to an agent less than 3 days before she becomes sYmptomatic and that every infected individual recovers with certainty after 100 days.

[34] Solving $(x/0.20)^0.12 = 0.5$ gives $x = 0.00062$, therefore we use this value

References

Acemoglu, Daron, Victor Chernozhukov, Iván Werning, and Michael D Whinston, "A Multi-Risk SIR Model with Optimally Targeted Lockdown," National Bureau of Economic Research 2020. (Cited on page 4)

Alfaro, Laura, Ester Faia, Nora Lamersdorf, and Farzad Saidi, "Social Interactions in Pandemics: Fear, Altruism, and Reciprocity," Technical Report, National Bureau of Economic Research 2020. (Cited on pages 3 and 4)

Alon, Titan M, Matthias Doepke, Jane Olmstead-Rumsey, and Michèle Tertilt, "The impact of COVID-19 on gender equality," *Covid Economics: Vetted and Real-Time Papers*, April 2020, *4*, 62–85. (Cited on page 31)

Alvarez, Fernando E, David Argente, and Francesco Lippi, "A simple planning problem for covid-19 lockdown," National Bureau of Economic Research 2020. (Cited on pages 4 and 31)

Antràs, Pol, Stephen J Redding, and Esteban Rossi-Hansberg, "Globalization and Pandemics," Technical Report, Harvard University Working Paper 2020. (Cited on page 4)

Atkeson, Andrew, "What will be the economic impact of COVID-19 in the US? Rough estimates of disease scenarios," National Bureau of Economic Research 2020. (Cited on page 4)

Aum, Sangmin, Sang Yoon Tim Lee, and Yongseok Shin, "COVID-19 Doesn't Need Lockdowns to Destroy Jobs: The Effect of Local Outbreaks in Korea," Technical Report, National Bureau of Economic Research 2020. (Cited on page 3)

Azzimonti, Marina, Alessandra Fogli, Fabrizio Perri, and Mark Ponder, "Social Distance policies in ECON-EPI networks," HEaLth and Pandemic webinar slides 2020. (Cited on page 4)

Barrios, John M, Efraim Benmelech, Yael V Hochberg, Paola Sapienza, and Luigi Zingales, "Civic Capital and Social Distancing during the Covid-19 Pandemic," Working Paper 27320, National Bureau of Economic Research June 2020. (Cited on page 3)

Bartik, Alexander W, Marianne Bertrand, Zoë B Cullen, Edward L Glaeser, Michael Luca, and Christopher T Stanton, "How are small businesses adjusting to covid-19? early evidence from a survey," Technical Report, National Bureau of Economic Research 2020. (Cited on page 3)

Bisin, Alberto and Andrea Moro, "Learning Epidemiology by Doing: The Empirical Implications of a Spatial SIR Model with Behavioral Responses," *Working paper, NYU and Vanderbilt*, 2020. (Cited on pages 2, 3, 5, 6, 9, 28, and 31)

_ **and** _ , "Notes on Rational Forward Looking SIR," mimeo, NYU 2020. (Cited on page 11)

Britton, Tom, Frank Ball, and Pieter Trapman, "A mathematical model reveals the influence of population heterogeneity on herd immunity to SARS-CoV-2," *Science*, 2020. (Cited on page 10)

Brotherhood, Luiz, Philipp Kircher, Cezar Santos, and Michèle Tertilt, "An economic model of the Covid-19 epidemic: The importance of testing and age-specific policies," *CEPR Discussion Paper No. DP14695*, 2020. (Cited on page 4)

Cicala, Steve, Stephen P Holland, Erin T Mansur, Nicholas Z Muller, and Andrew J Yates, "Expected Health Effects of Reduced Air Pollution from COVID-19 Social Distancing," Working Paper 27135, National Bureau of Economic Research May 2020. (Cited on page 3)

Coibion, Olivier, Yuriy Gorodnichenko, and Michael Weber, "The cost of the covid-19 crisis: Lockdowns, macroeconomic expectations, and consumer spending," Technical Report, National Bureau of Economic Research 2020. (Cited on page 3)

Dingel, Jonathan I. and Brent Neiman, "How Many Jobs Can Be Done at Home?," Mimeo, U. of Chicago 2020. (Cited on pages 11 and 31)

Eichenbaum, Martin S, Sergio Rebelo, and Mathias Trabandt, "The macroeconomics of epidemics," National Bureau of Economic Research 2020. (Cited on page 4)

Ellison, Glenn, "Implications of Heterogeneous SIR Models for Analyses of COVID-19," National Bureau of Economic Research Working Paper 27373 June 2020. (Cited on page 4)

Eubank, Stephen, Hasan Guclu, VS Anil Kumar, Madhav V Marathe, Aravind Srinivasan, Zoltan Toroczkai, and Nan Wang, "Modelling disease outbreaks in realistic urban social networks," *Nature*, 2004, *429* (6988), 180–184. (Cited on page 2)

Ferguson, Neil, Daniel Laydon, Gemma Nedjati Gilani, Natsuko Imai, Kylie Ainslie, Marc Baguelin, Sangeeta Bhatia, Adhiratha Boonyasiri,

ZULMA Cucunuba Perez, Gina Cuomo-Dannenburg et al., "Imperial College COVID-19 Response Team: Impact of non-pharmaceutical interventions (NPIs) to reduceCOVID-19 mortality and healthcare demand," Imperial College London 2020. (Cited on pages 6, 10, 30, and 31)

Fernandez-Villaverde, Jesus and Charles Jones, "Estimating and Simulating a SIRD Model of COVID-19," mimeo 2020. (Cited on page 4)

Gans, Joshua S, "The Economic Consequences of $\hat{R} = 1$: Towards a Workable Behavioural Epidemiological Model of Pandemics," Working Paper 27632, National Bureau of Economic Research July 2020. (Cited on page 11)

Glaeser, Edward L, Caitlin S Gorback, and Stephen J Redding, "How Much does Covid-19 Increase with Mobility? Evidence from New York and Four Other U.S. Cities," mimeo 2020. (Cited on page 4)

Gomes, M Gabriela M, Ricardo Aguas, Rodrigo M Corder, Jessica G King, Kate E Langwig, Caetano Souto-Maior, Jorge Carneiro, Marcelo U Ferreira, and Carlos Penha-Goncalves, "Individual variation in susceptibility or exposure to SARS-CoV-2 lowers the herd immunity threshold," *medRxiv*, 2020. (Cited on page 10)

Goolsbee, Austan and Chad Syverson, "Fear, lockdown, and diversion: comparing drivers of pandemic economic decline 2020," Technical Report, National Bureau of Economic Research 2020. (Cited on page 3)

Gupta, Sumedha, Laura Montenovo, Thuy D Nguyen, Felipe Lozano Rojas, Ian M Schmutte, Kosali I Simon, Bruce A Weinberg, and Coady Wing, "Effects of social distancing policy on labor market outcomes," Technical Report, National Bureau of Economic Research 2020. (Cited on page 3)

Jarosch, Gregor, Maryam Farboodi, and Robert Shimer, "Internal and External Effects of Social Distancing in a Pandemic," 2020. (Cited on page 4)

Kahn, Lisa B, Fabian Lange, and David G Wiczer, "Labor Demand in the Time of COVID-19: Evidence from Vacancy Postings and UI Claims," Working Paper 27061, National Bureau of Economic Research April 2020. (Cited on page 3)

Kaplan, Greg, Ben Moll, and Gianluca Violante, "Pandemics According to HANK," *University of Chicago*, 2020. (Cited on pages 4 and 31)

Keppo, Juusi, Marianna Kudlyak, Elena Quercioli, Lones Smith, and Andrea Wilson, "The behavioral SIR model, with applications to the Swine Flu and COVID-19 pandemics," in "Virtual Macro Seminar" 2020. (Cited on pages 4, 10, 11, and 31)

Kermack, William Ogilvy and Anderson G McKendrick, "A contribution to the mathematical theory of epidemics," *Proceedings of the royal society of london. Series A, Containing papers of a mathematical and physical character*, 1927, *115* (772), 700–721. (Cited on page 2)

_ and _ , "Contributions to the mathematical theory of epidemics. II. -The problem of endemicity," *Proceedings of the Royal Society of London. Series A, containing papers of a mathematical and physical character*, 1932, *138* (834), 55–83. (Cited on page 2)

Kindermann, R and JL Snell, "American Mathematical Society," *Markov random fields and their applications*, 1980. (Cited on page 6)

Liggett, Thomas Milton, *Interacting particle systems*, Vol. 276, Springer Science & Business Media, 2012. (Cited on page 6)

Lucas, Robert E, "Econometric policy evaluation: A critique," in "Carnegie-Rochester conference series on public policy," Vol. 1 1976, pp. 19–46. (Cited on pages 4 and 23)

Mossong, Joël, Niel Hens, Mark Jit, Philippe Beutels, Kari Auranen, Rafael Mikolajczyk, Marco Massari, Stefania Salmaso, Gianpaolo Scalia Tomba, Jacco Wallinga, and et al., "Social Contacts and Mixing Patterns Relevant to the Spread of Infectious Diseases," *PLoS Medicine*, Mar 2008, *5* (3), e74. (Cited on pages 6, 9, and 29)

Rojas, Felipe Lozano, Xuan Jiang, Laura Montenovo, Kosali I Simon, Bruce A Weinberg, and Coady Wing, "Is the cure worse than the problem itself? immediate labor market effects of covid-19 case rates and school closures in the us," Technical Report, National Bureau of Economic Research 2020. (Cited on page 3)

Weitz, Joshua S, Sang Woo Park, Ceyhun Eksin, and Jonathan Dushoff, "Moving Beyond a Peak Mentality: Plateaus, Shoulders, Oscillations and Other'Anomalous' Behavior-Driven Shapes in COVID-19 Outbreaks," *medRxiv*, 2020. (Cited on page 4)